Resonant-Wavelength Control and Optical-Confinement Analysis for Graded SCH VCSELs Using a Self-Consistent Effective-Index Method

Wei-Choon Ng, *Member, IEEE*, Yang Liu, and Karl Hess, *Fellow, IEEE*

***Abstract*—We report novel design considerations for graded separate confinement heterostructure (SCH) cavities of oxide-confined vertical-cavity surface-emitting lasers (VCSELs). Using a self-consistent effective-index method, we have analyzed ungraded, linearly and exponentially graded SCH cavities of an 850-nm VCSEL. An ungraded SCH gives the best optical-confinement factor, while linear and exponential gradings reduce the factor by 18% and 9%, respectively. Grading the SCH cavities of oxide-confined VCSELs leads to both a shift in the resonant wavelength as well as a decrease in the optical-confinement factor. The resonant-wavelength shifts in graded SCH cavities are attributed to two competing effects: the formation of an effective-index step that redefines the λ cavity, and larger optical-field leakage, which relaxes the confinement. We have also demonstrated that wavelength shifts can be easily compensated by optimized width extensions of the aperture layers which sandwich the graded SCH cavity, without further reducing the optical-confinement factor. Based on a revised understanding of the resonances for graded SCH cavities, we can therefore control the design of graded SCH VCSELs to obtain a desired resonant wavelength with great precision.**

***Index Terms*—Effective-index method (EIM), GRIN separate confinement heterostructure, optical confinement, resonance, vertical-cavity surface-emitting lasers (VCSELs).**

I. Introduction

VERTICAL-cavity surface-emitting lasers (VCSELs) are important components for short-range optical communications. Of great promise are oxide-confined VCSELs, which achieve both transverse optical and carrier confinements by a single oxidation step [1]. The channels in dense wavelength-division multiplexing systems are just nanometers apart. Hence, the exact control of resonant wavelengths becomes a crucial issue in oxide-confined VCSELs. Furthermore, due to the small gain volume, it is important to confine the optical-field intensity as much as possible to the quantum wells (QWs) in order to achieve maximum modal gain.

A separate confinement heterostructure (SCH) is commonly used for optical confinement in the vertical direction. In edge-emitting laser diodes, one can achieve an optimum vertical-optical-confinement factor by varying the width of the waveguiding layers within the SCH [2]. As the width of the guiding layers is reduced, the optical mode is squeezed until it begins to leak through the guiding layers, hence limiting the optical-confinement factor. If the SCH is graded, then a larger optical guide thickness is required [3]. In VCSELs, however, the SCH cavity is constrained to be equal to the wavelength λ, so that the fundamental mode resonance is established about λ. The only available design freedom is the grading of guiding layers within the SCH, while maintaining the entire width of the SCH cavity to be effectively 1λ thick. It is advantageous from the electronic-transport perspective to grade the SCH cavity, because the grading provides an additional electric field, which helps in collecting the charge carriers in the quantum wells. Grading also results in a lower density of states in the confining region above the well [4]. However, graded guiding layers cause further leakage of the optical field out of the SCH cavity, leading to a reduction of the optical-confinement factor in the QWs. As a first comparison, an ungraded SCH can exhibit an 18% larger optical-confinement factor compared to a linearly graded SCH. We have also found that the resonant wavelength is shifted by a few nanometers, even if we constrain the graded SCH cavity to have an effective thickness of 1λ. This shift is caused by competing effects of a shift in an effective-confinement boundary as well as a larger leakage of the optical field. This leads to new design considerations for graded SCH VCSELs (a resonator problem), which are different from those of edge-emitters (a waveguide problem). In addition to the resonant wavelength shift caused by grading, reducing the size of the oxide aperture also causes a blue shift [5]. We will show that such resonant-wavelength shifts can be easily compensated, without lessening the optical-confinement factor, by increasing the width of the aperture layers that sandwich the graded SCH cavity. Hence, we can control the resonant wavelength to the desired value with great precision. In order to further understand the physics of the SCH resonator design, we examine linearly and exponentially graded SCH structures for oxide-confined VCSELs. Generic VCSEL structures with different numbers of QWs and lasing at 850 nm are systematically investigated.

Optical simulation of oxide-confined VCSELs is a nonlinear problem in frequency ω. Accurate vector methods such as finite-difference, finite-element, and Green's function methods are computationally intensive and thus impede fast prototyping

Manuscript received April 22, 2002; revised October 9, 2002. This work was supported by the Office of Naval Research Contract N0014-98-1-0604.

The authors are with the Beckman Institute, University of Illinois, Urbana, IL 61801 USA (e-mail: weichoon@ieee.org).

Digital Object Identifier 10.1109/JLT.2003.808758

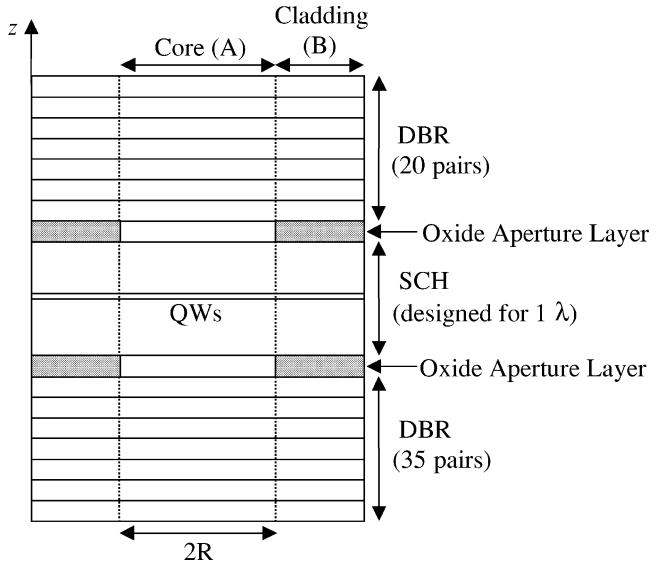

Fig. 1. General geometry of an oxide-confined VCSEL structure used by the S-EIM. The SCH cavity is sandwiched by two aperture layers, where the oxide apertures are formed. 20 and 35 pairs of DBR mirrors are formed at the top and bottom of the SCH cavity, respectively. The diameter of the aperture is $2R$.

and analysis. Recently, we have shown that our self-consistent effective-index method (S-EIM) is able to compute resonant wavelengths and optical mode profiles of oxide-confined VCSELs accurately compared to the vector Green's function method [6] and experimental results [7]. Furthermore, the S-EIM elucidates the physics of resonances in VCSELs and thus provides a comprehensive tool for optical analysis. Therefore, we use the S-EIM for the optical-confinement analysis and resonant-wavelength control of oxide-confined VCSELs in this work.

The organization of the paper is as follows. The theory and physics behind the S-EIM will be discussed briefly in Section II. In Section III, we analyze three graded SCH models of oxide-confined VCSELs to understand how one can control the resonant wavelength and the optical confinement.

II. Theory of the S-EIM

Many variants of the EIM [8]–[11] exist and have been applied to the analysis of VCSELs. The first approach was proposed by Hadley [8]. In the EIM formulations of Hadley [8] and Yu [9], a time variation is involved and the authors have assumed a slowly varying envelope function to derive a beam-propagation-type equation. Hegblom *et al.* [12] has also formulated a beam-propagation-type equation with distributed effective indexes based on the classic work of Fox and Li [13]. On the other hand, Wenzel's effective-frequency method [10] is based on a complex variational functional from which he established effective frequencies for each region to include dispersion effects. Our S-EIM is a novel variant of the EIM that also takes dispersion effects into consideration. These are implemented in a self-consistent and physically intuitive manner.

Fig. 1 shows the VCSEL structure which can be modeled by the S-EIM. We consider only two regions, the core (A) and the cladding (B) region, for simplicity in outlining the S-EIM. We can, however, divide the transverse plane into more regions if necessary. In each region, we allow for a multilayered stack composed of homogeneous layers with different refractive indexes. We wish to approximate the solution to the scalar wave equation

$$\nabla^2\psi + k^2\psi = 0 \tag{1}$$

where ψ denotes a transverse component of the electric field. Assuming separability of the wavefunction $\psi = \phi_t(x,y)\phi_z(z)$, we can partition the Laplacian into its transverse (subscript t) and z components, leading to the transverse and the axial wave equations

$$\left[\nabla_t^2 + k_t^2\right]\phi_t = 0 \tag{2}$$

$$\left[\frac{\partial^2}{\partial z^2} + k_z^2\right]\phi_z = 0. \tag{3}$$

These are coupled to each other via the dispersion relation

$$\begin{aligned} k^2 &= k_t^2 + k_z^2 \\ &= \omega^2\mu\epsilon \\ &= n^2 k_0^2 \end{aligned} \tag{4}$$

where $k_0 = 2\pi/\lambda_0$. ω and λ_0 are the resonant frequency and wavelength of the VCSEL structure, respectively. In each layer i of the core region A, the solution to (3) can be expressed as the sum of a forward and backward propagating wave

$$\phi_z = A_i \exp(\mathrm{ik_{zi}}z) + B_i \exp(-\mathrm{ik_{zi}}z). \tag{5}$$

A cascaded matrix can be formed which relates the field at the top edge to that of the bottom edge of the device by matching boundary conditions. We vary the frequency ω and a gain variable in the QWs until only outward-propagating waves are established at the top and bottom edges of the device. Physically, the gain in the QWs balances the radiative losses out of the device. At this instance, resonance is established and we obtain the z-resonant field intensity. Assuming that this z-resonant field is dominant, we use it to compute the effective indexes for the core and cladding regions

$$n_{\mathrm{core/clad}}^2 = \frac{\sum_i \int_{z_i}^{z_{i+1}} n_i^{(A/B)2}|\phi_z|^2 dz}{\int |\phi_z|^2 dz}. \tag{6}$$

If we had used more than two regions, we would compute the effective indexes of the other regions similarly. These effective indexes are used in (2) to solve an optical-fiber-type problem [14]. If we substitute (3) into (1) and then take the closed product of the equation with ϕ_z, we recover (2) with

$$k_t^2 = n_{\mathrm{core(clad)}}^2 k_0^2 - \beta^2 \tag{7}$$

where β is the propagation constant for the optical-fiber-type problem. To better understand the physics of wave propagation in such a device, assume a plane wave propagating through the device. The oxide aperture or transverse inhomogeneities cause diffraction of the plane wave, and the diffraction effect changes the transverse phase k_t. Using the effective indexes and solving the optical-fiber-type problem, an average diffraction effect is computed in the form of an average transverse phase change in

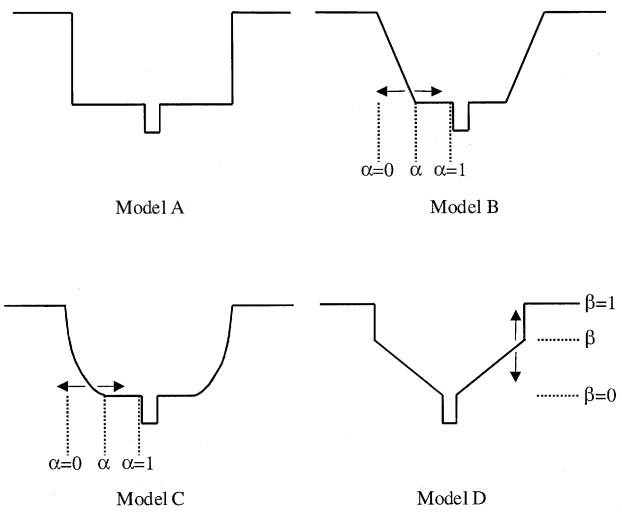

Fig. 2. Grading profile for the SCH cavity is represented by its conduction-band variation. Model A is ungraded. Models B and D are linearly graded, while model C is exponentially graded. α denotes the extent of grading from the SCH edge to the QWs for models B and C. β denotes the amount of discontinuity for model D.

(7). The average transverse phase number k_t must be constant in all the layers by the concept of phase matching. Therefore, substituting (7) into (4) to solve for k_z in each layer, the average transverse phase k_t is incorporated in all layers. The solution process is iterated alternately until all the physics of the structure are self-consistently satisfied. Computing the resonant wavelength, threshold gain, and resonant-mode profile are extremely fast, and takes less than 10 s on a 350-MHz PC.

As a further note, Serkland [11] has used the same time harmonic equations as we have. However, the key difference in his formulation is that he has assumed $n_{\text{core}} = n_{\text{clad}}$ with two different resonant frequencies for the core and cladding regions before solving the optical-fiber-type problem.

III. Results and Discussions

We use generic oxide-confined VCSEL structures which contain 20 upper and 35 lower distributed Bragg reflector (DBR) pairs and a SCH cavity that has four different gradings, as shown in Fig. 2 [15]. Model A is an ungraded SCH cavity. We define a parameter $\alpha(0 \leq \alpha \leq 1)$ for models B and C that denotes the extent of linear and exponential grading from the edge of the SCH toward the QWs. $\alpha = 0$ means zero grading and $\alpha = 1$ denotes the grading extends up to the QWs. Similarly, we define $\beta(0 \leq \beta \leq 1)$ for model D such that $\beta = 0$ depicts zero grading and $\beta = 1$ gives a grading that extends from the edge of SCH. A dense staircase approximation is used for the linear and exponential grading profiles. The cavity design requires imposing the constraint that the effective optical length of the SCH cavity must add up to 1λ, $\sum_i n_i L_i = \lambda_0$, where n_i and L_i are the refractive index and thickness of each layer in the SCH cavity, and λ_0 is the desired freespace resonant wavelength. The QWs are designed to lase at 850 nm, and Table I summarizes the materials used for the 850 nm VCSEL. The refractive indexes of $Al_xGa_{1-x}As$ are directly interpolated from experimental values [16].

TABLE I
Materials Used for Various Components of an 850-nm Oxide-Confined VCSEL

Component	Material, Thickness
Each DBR-pair	$Al_{0.1}Ga_{0.9}As - Al_{0.9}Ga_{0.1}As, \lambda/4$
Oxide aperture layer	$Al_{0.98}Ga_{0.02}As, \lambda/4$
QWs	$GaAs, 80$Å
QW barrier	$Al_{0.2}Ga_{0.8}As, 80$Å

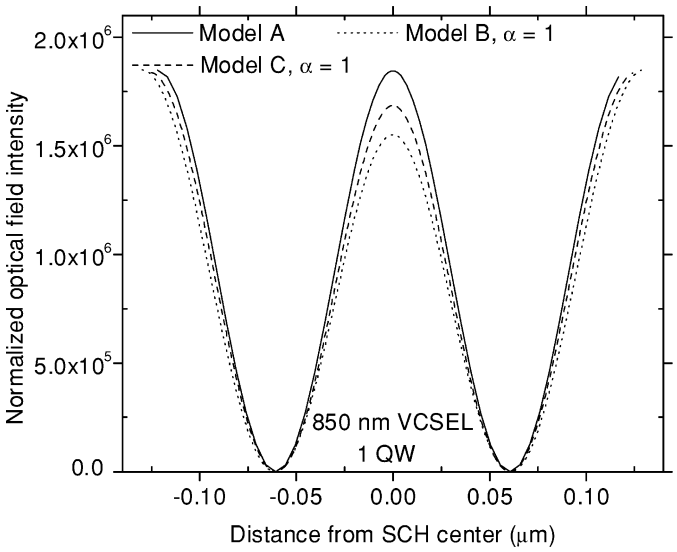

Fig. 3. Comparison of the normalized resonant-field intensity $\left(|\phi_z|^2 / \int_z |\phi_z|^2 dz\right)$ within the SCH cavity for three different graded SCH cavities. The resonance is designed for 850 nm.

The normalized resonant optical-field intensities within the SCH cavity for the ungraded (model A), linearly (model B, $\alpha = 1$) and exponentially (model C, $\alpha = 1$) graded SCH models of an 850-nm VCSEL are plotted in Fig. 3. It is evident that the leakage of the optical field out of the SCH cavity is largest for model B. Such leakage cannot be reduced by increasing the number of DBR mirror pairs because the reflection occurs over a distributed distance. The SCH cavity as well as the $\lambda/4$ layers very close to it hold the key to controlling the optical confinement. Here, we emphasize the SCH cavity only. The larger optical leakage out of the SCH cavity leads to a reduction of the optical-confinement factor as well as a change in the resonant wavelengths. Our following analysis reveals competing factors which cause the resonant wavelength shifts.

Fig. 4 shows the resonant wavelengths λ_0 plotted as a function of α (models B and C) and β (model D), the extent of linear and exponential grading in the SCH cavity. It is well known that reducing the aperture radius causes a blue-shift in λ_0 [5]. This is due to increased optical-field interaction with smaller oxide apertures, which causes a stronger diffraction effect. In Section II, we have clarified that the diffraction effect results in a transverse phase shift, which subsequently alters the resonance of the device. The λ_0 curves in Fig. 4 only translate

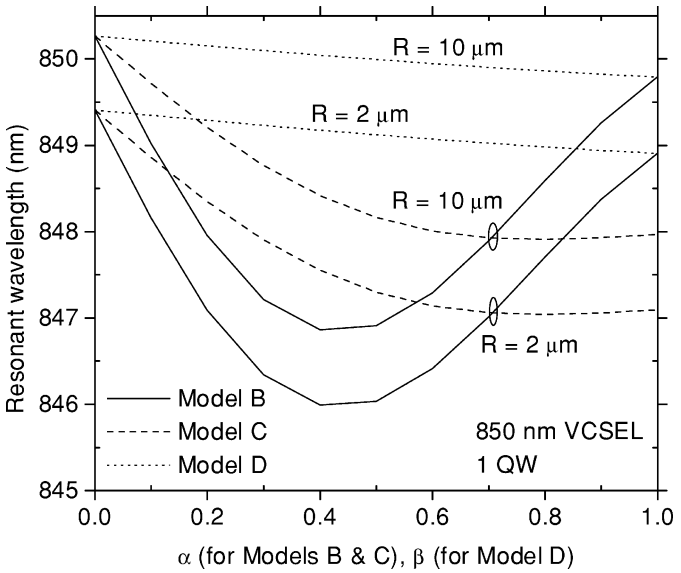

Fig. 4. Resonant wavelengths of an 850-nm VCSEL with linearly and exponentially graded SCH cavities plotted against the extent of grading α for models B and C and β for model D.

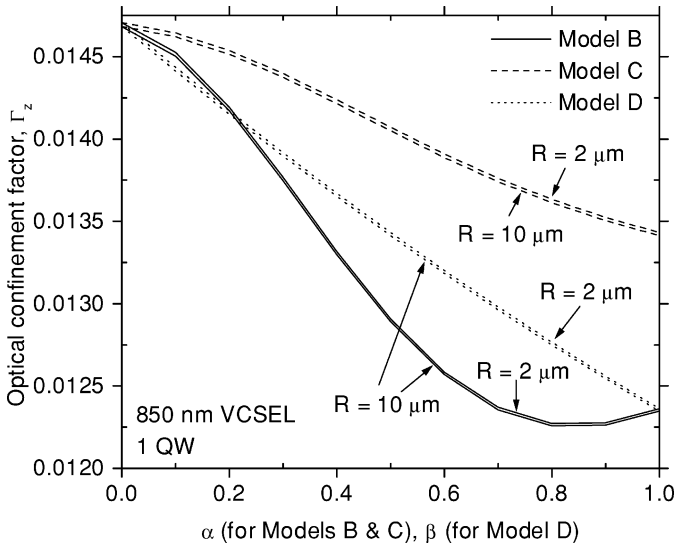

Fig. 5. Optical-confinement factors of an 850-nm VCSEL with linearly and exponentially graded SCH cavities plotted against the extent of grading α for models B and C and β for model D.

upwards when the aperture radius is increased. Therefore, the larger leakage of optical field due to the grading has negligible effect of causing such λ_0 variations via interaction with the oxide aperture. In order to understand the physics behind the λ_0 variations, we have to reconsider the definition of a 1λ cavity. Such a cavity is formed by a sharp and large refractive-index step difference at the edge of the SCH. If the SCH is graded, then we will have to consider an effective refractive-index step that redefines the λ cavity confinement boundary. As the grading for models B and C moves toward the QWs, the effective-index step shifts toward the QWs and is no longer at the edge of the SCH cavity. This results in a smaller effective cavity and hence reduces λ_0. We have a competing effect for model B that has a linear grading. As α increases, the slope of the linear grading decreases, leading to a reduction in the size of the effective-index step. The reduced effective-index step relaxes the confinement and allows larger optical leakage, resulting in an increase in λ_0. This competing effect becomes increasingly comparable to the effect of effective-confinement boundary shift at larger α values. As a result, we obtain the U-shape λ_0 variation for model B in Fig. 4. On the other hand, the step discontinuity in model D helps to define the λ cavity at the edge of the SCH. As β approaches 1, the step discontinuity diminishes and leads to the formation of an effective-index step that moves inwards. At the same time, the reduced effective-index step relaxes the confinement ability. The two competing effects for model D (with varying β) are comparable, so the λ_0 shift is minimal.

The longitudinal optical-confinement factors Γ_z are plotted as a function of the extent of linear and exponential SCH grading in Fig. 5. As the grading extends further toward the QWs, Γ_z decreases for all the graded models. The difference in Γ_z between an ungraded (model A) and a linearly graded SCH (model B, $\alpha = 1$) can be as large as 18%. The decrease of Γ_z for the linearly graded models B and D is much larger than for the exponentially graded model C, as observed from Fig. 5. Model C provides a larger effective-index step than the linearly graded models B and D, hence reducing the optical-field leakage and resulting in a smaller reduction of the optical-confinement factor. On the other hand, as shown in Fig. 5, changing the aperture radius only changes the longitudinal optical-confinement factor negligibly.

Two simple ways exist to compensate the blue-shifts in λ_0 for graded SCH cavities. The first is to reduce the Al ratio (increasing the refractive index) of the oxide-aperture layer so that the index-step difference is decreased. This allows larger optical-field leakage and a larger effective cavity for red shifts in λ_0. However, in doing so, we have reduced the optical-confinement factor further. The second way is to add buffer layers at the edge of the SCH cavity so that we have a larger than 1λ cavity

$$\sum_i n_i L_i = (1+\kappa)\lambda_0 \tag{8}$$

where κ can be called a resonance-ideality factor, which is adjusted to set the resonance to exactly λ_0. In this case, we do not allow larger optical leakage out of the SCH cavity, and hence, will not decrease the optical-confinement factor. The buffer layers can simply be chosen as width extension of the aperture layers by $\kappa\lambda_0/n_{\text{aperture}}$. Negative and positive κ give blue and red shifts in λ_0, respectively. We can therefore control the resonant wavelength to a desired design value with great precision. In Fig. 6, we show that this method can also be used to compensate the blue-shifts caused by smaller aperture radius, so that the resonance is maintained at exactly 850 nm. The addition of a spacer layer after the SCH cavity has been formed is also a common method used by VCSEL growers to tune the resonance of the SCH cavity. This may, however, lead to misalignment of the resonant-field peak with the QWs. Our proposed resonance-ideality factor would serve as a good guideline on the correct thickness of the compensating spacer layers required on both ends of the SCH cavity to ensure that the resonant-field peak aligns with the QWs.

Fig. 7 shows the resonance-ideality factor κ required to set the resonance of multiple QWs VCSELs to exactly 850 nm. The set

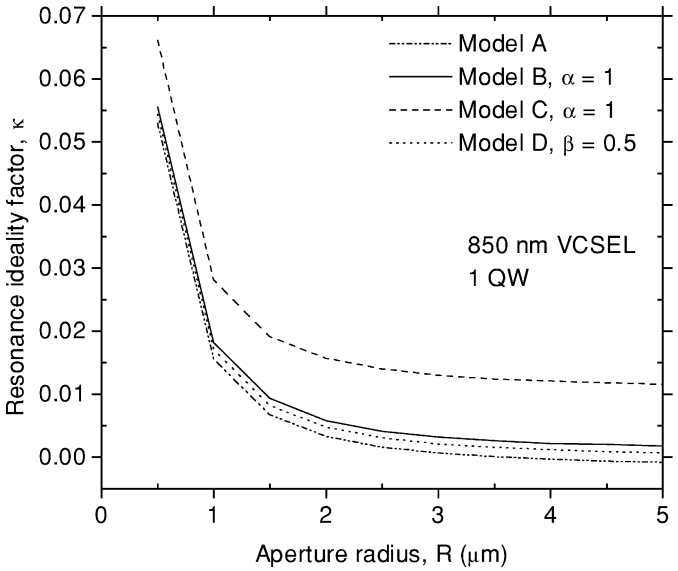

Fig. 6. Resonance-ideality factor κ for aperture-layer width extension can be adjusted to compensate the blue-shifts caused by aperture size (radius R) reduction so that the resonant wavelength is maintained at 850 nm.

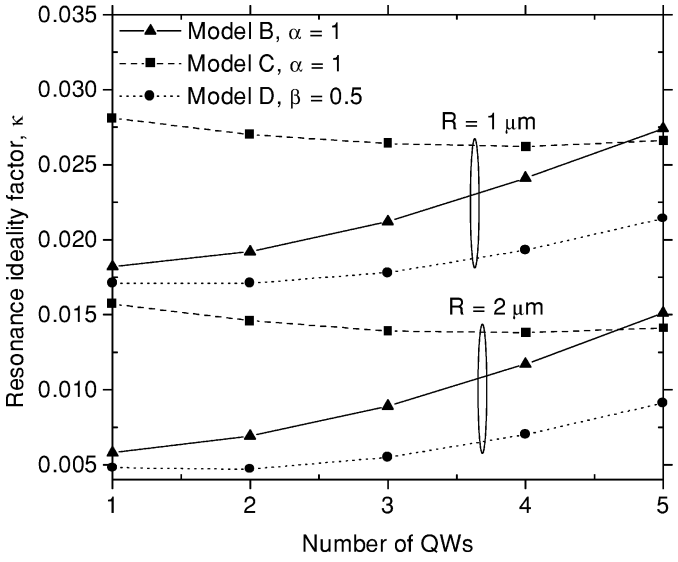

Fig. 7. Resonance-ideality factor κ, needed to ensure that the resonant wavelength of multiple QWs VCSEL is maintained at 850 nm, for three different graded-SCH cavities.

of curves translate vertically for different aperture radii, while their variations are due to changes in the grading region. When we increase the number of QWs, the width of the grading region is reduced. This is equivalent to reducing α, the extent of grading for the SCH models that we have previously examined in Fig. 4. Therefore, the κ values for increasing number of QWs (as shown in Fig. 7) vary correspondingly to the wavelength shifts caused by reducing α. We also compare the longitudinal optical-confinement factors Γ_z of the various SCH models with multiple QWs in Fig. 8. Model A (ungraded) offers the best optical-confinement, factor but it does not provide the electronic transport advantage of a graded SCH. A compromise would be to choose an exponential grading (model C), which offers a 10% greater optical-confinement factor than a full linear grading. Alternatively, we could also select model D with $\beta < 0.5$. For longer

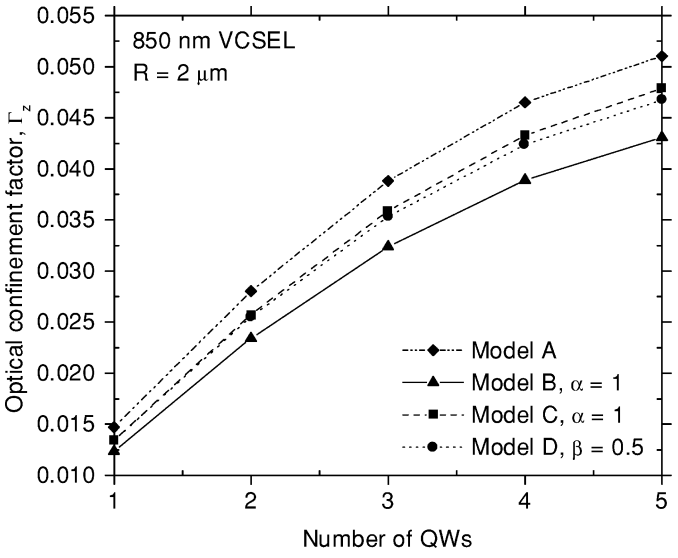

Fig. 8. Optical-confinement factors of ungraded and graded SCH VCSELs for 850 nm plotted as a function of the number of QWs. The resonant wavelength has been adjusted to 850 nm by varying κ.

wavelength VCSELs, we expect the λ cavity to become wider and the optical field to be more widespread. This results in further reduction of the optical-confinement factor. Therefore, the choice of grading in the SCH cavity becomes more important for long-wavelength VCSELs, and the analysis presented here may serve as a guide.

IV. Conclusion

We have demonstrated that grading the SCH cavities of oxide-confined VCSELs leads to resonant-wavelength shifts and reduction of the optical-confinement factor. The resonant-wavelength shifts in graded SCH cavities are attributed to two competing effects: the inward shift of an effective-index step, which redefines the λ cavity confinement boundary, and the reduction of the effective-index step, leading to relaxed confinement abilities of the λ cavity. The former effect causes a reduction in λ_0, while the latter effect increases λ_0. Therefore, new design considerations that are different from those of edge-emitters have to be formulated for the VCSEL resonator problem with graded SCH cavities. We have also shown that a linearly graded SCH leads to as much as 18% reduction in the optical-confinement factor as compared to an ungraded SCH for a 850-nm VCSEL. A compromise would be to use an exponential grading that provides a larger effective-index step for better optical-confinement factor and maintains the advantage for electronic transport.

Based on the understanding gained from the analysis in this work, we have proposed a simple method to compensate resonant-wavelength shifts caused by grading the SCH and aperture-size reduction. The λ_0 shifts can be compensated by extending the width of the aperture layer by an amount of $\kappa\lambda_0/n_{\text{aperture}}$, where κ is the resonance-ideality factor. This ensures that the resonant wavelength can be adjusted to achieve the desired value without further reducing the optical-confinement factor. Computing κ entails repeated optical simulations of changing VCSEL geometry and, hence, a fast optical solver is needed. In this respect, the S-EIM becomes an ideal tool to

facilitate the analysis and design of graded SCH oxide-confined VCSELs with precise control of the resonant wavelength.

ACKNOWLEDGMENT

The authors would like to thank Prof. K. D. Choquette, University of Illinois, Urbana, for valuable discussions on geometries of oxide-confined VCSELs. They would also like to thank the reviewers for their constructive comments.

REFERENCES

[1] K. D. Choquette, R. P. Schneider, K. L. Lear, and K. M. Geib, "Low threshold voltage vertical-cavity lasers fabricated by selective oxidation," *Electron. Lett.*, vol. 30, pp. 2043–2044, 1994.

[2] S. R. Chinn, "Modal analysis of GRIN-SCH and triangular-well waveguides," *Appl. Opt.*, vol. 23, pp. 3508–3509, Oct. 1984.

[3] D. P. Bour, "AlGaInP quantum well lasers," in *Quantum Well Lasers*, P. S. Zory, Ed. New York: Academic, 1993, ch. 9.

[4] J. Nagle, S. Hersee, M. Krakowski, T. Weil, and C. Weisbuch, "Threshold current of single quantum well lasers: The role of the confining layers," *Appl. Phys. Lett.*, vol. 49, no. 20, pp. 1325–1327, Nov. 1986.

[5] M. J. Noble, J. H. Shin, K. D. Choquette, J. P. Loehr, J. A. Lott, and Y. H. Lee, "Calculation and measurement of resonant-mode blueshifts in oxide-apertured VCSELs," *IEEE Photon. Technol. Lett.*, vol. 10, pp. 475–477, Apr. 1998.

[6] B. Klein, L. F. Register, K. Hess, D. G. Deppe, and Q. Deng, "Self-consistent Green's function approach to the analysis of dielectrically apertured vertical-cavity surface-emitting lasers," *Appl. Phys. Lett.*, vol. 73, no. 23, pp. 3324–3326, Dec. 1998.

[7] W. C. Ng, Y. Liu, B. Klein, and K. Hess, "Improved effective index method for oxide-confined VCSEL mode analysis," *Proc. SPIE*, vol. 4646, pp. 168–175, 2002.

[8] G. R. Hadley, "Effective index model for vertical-cavity surface-emitting lasers," *Opt. Lett.*, vol. 20, pp. 1483–1485, 1995.

[9] S. F. Yu, "Dynamic behavior of vertical-cavity surface-emitting lasers," *IEEE J. Quantum Electron.*, vol. 32, pp. 1168–1179, July 1996.

[10] H. Wenzel and H. J. Wunsche, "The effective frequency method in the analysis of vertical-cavity surface-emitting lasers," *IEEE. J. Quantum Electron.*, vol. 33, pp. 1156–1162, July 1997.

[11] D. K. Serkland, G. R. Hadley, K. D. Choquette, K. M. Geib, and A. A. Allerman, "Modal frequencies of vertical-cavity lasers determined by an effective-index model," *Appl. Phys. Lett.*, vol. 77, no. 1, pp. 22–24, July 2000.

[12] E. R. Hegblom, D. I. Babic, B. J. Thibeault, and L. A. Coldren, "Scattering losses from dielectric apertures in vertical-cavity lasers," *IEEE J. Select. Topics Quantum Electron.*, vol. 3, pp. 379–389, Apr. 1997.

[13] A. G. Fox and T. Li, "Resonant modes of a maser interferometer," *Bell Syst. Technol. J.*, vol. 40, pp. 453–473, 1961.

[14] A. W. Synder and J. D. Love, *Optical Waveguide Theory*. London, U.K.: Chapman and Hall, 1983.

[15] K. D. Choquette, private communication.

[16] S. Adachi, "Optical properties of AlGaAs: Transparent and interband-transition regions (tables)," in *Properties of Aluminum Gallium Arsenide*, S. Adachi, Ed. New York: IEE, 1993, ch. 5.5.

Wei-Choon Ng (S'98–M'03) received the B.Eng. degree (with first class honors) and the M.Eng. degree in electrical engineering from the National University of Singapore in 1996 and 1998, respectively, and the Ph.D. degree in electrical engineering from the University of Illinois at Urbana—Champaign in 2002.

In 1995, he worked on optical thin-film coating in British Telecoms Labs, Ipswich, U.K., for his industrial placement. He was a Graduate Research Assistant with the Computational Electronics Group at the University of Illinois from 1999 to 2002. He is currently a Development Engineer with Integrated Systems Engineering, San Jose, CA. His research interests mainly focus on semiconductor transport, thermal modeling of semiconductor lasers, modeling guided-wave devices, and computational electromagnetics.

Dr. Ng is a Member of the IEEE Lasers and Electro-Optic Society (LEOS) and Phi Kappa Phi and is a Senior Research Fellow of the International Society for Philosophical Enquiry (ISPE).

Yang Liu received the B.S. degree in physics from the University of Science and Technology of China, Hefei, in 1998 and the Ph.D. degree in physics from the University of Illionis at Urbana—Champaign in 2002.

His major interests include semicondutor device physics and the modeling and simulation of optoelectronics.

Karl Hess (F'85) received the Ph.D. degree in applied physics from the University of Vienna, Vienna, Austria, in 1970.

Currently, he holds the Swanlund Endowed Chair and is a Professor of electrical and computer engineering and of physics at the University of Illinois at Urbana-Champaign. He has dedicated the major portion of his research to electronic transport in semiconductors and semiconductor devices, with particular emphasis on hot electron effects and effects pertinent to device miniaturization. He is particularly interested in problems that require large computational resources for their solution. His current research at the Beckman Institute, University of Illinois, is in the area of molecular and electronic nanostructures.

Dr. Hess has received numerous awards, including the IEEE J.J. Ebers Award of the Electron Devices Society (EDS) in 1993 and the IEEE Sarnoff Field Award for Electronics in 1995. He is a Fellow of the APS, the AAS, and the American Academy of Arts and Sciences, and a Member of the National Academy of Engineering.